23rd Australasian Fluid Mechanics Conference – 23AFMC
Sydney, Australia
4-8 December 2022
Paper No: AFMC2022-285

Prediction of Store Separation Trajectories of the Eglin Test Model using Cradle CFD

Ganesh Pawar R [1*], Nuza Nigar [1,2], Praphul T. [1], Dr. Karthik Sundarraj [1]

[1] Hexagon Manufacturing Intelligence, Bangalore, Karnataka – 560043, India

[2] University of Petroleum and Energy Studies, Dehradun, Uttarakhand – 248007, India

* Email: ganesh.pawar@hexagon.com

Abstract

Testing of store separation involves risk and could result in fatal accidents. It also involves a huge testing cost. The traditional use of flight tests and Wind Tunnel Testing required very long testing time. With the development of Computational Fluid Dynamics, it has become easier to simulate the store separation. To establish this, the coupling of Six DOF equations with the Navier Stokes equations is needed. The force and moments on a store can be calculated using CFD applied to the wing, pylon, and store geometry. The purpose of this project is to use Software Cradle to validate the store separation trajectory using the Eglin Test Model. This work also presents detailed attention to the ejector force profile. The transonic Mach number for which the simulation is performed is 0.95. The software Cradle's scFLOW code is used to solve the Reynolds Averaged Navier Stokes Equation which is coupled with the 6 Degree of Freedom Equation. The overset meshing technique is employed. The simulation results in good agreement with the Linear and Angular Displacement of the store.

1. Introduction

The separation of the store from the air vehicle is a critical issue in terms of the missile integration process. Whenever a store separates from the aircraft during flight it is extremely required that it does not come in contact with the aircraft.(Demir et al., n.d.) Traditionally, flight tests were performed to test the store separation, however, they were very time-consuming and often required years to certify a projectile.(Panagiotopoulos & Kyparissis, n.d.) In the 1960s, Wind Tunnel Testing was done to perform the store separation tests. However, such testing had long lead times and limited accuracy. The method used in such a wind tunnel was the Captive Trajectory System. However, the CTS system had no accuracy in time. Thus, they do not account for the inherent unsteadiness encountered by the store during separation. Also, due to the use of small-scale models, scaling problems often lead to a reduction in accuracy.(Madasamy S et al., 2016) The development of High Parallel Computing and numerical algorithms have paved a safe path to numerical solutions for Store Separation. Such numerical modelling and simulations have reduced the certification cost and increased the margin of safety of flight tests. Trajectories of stores released from internal weapons bays have been shown in recent tests to diverge from predicted paths. It is critical to develop an accurate method of predicting the trajectory of a transonic regime especially. In a transonic regime, a complex transient interaction phenomenon exists, which when must be simulated, needs to consider the compressibility effects and the strong interference flow fields that are generated between the wing and pylon and the store body.

However, the challenge of CFD is to provide accurate data on time. The computation cost increases due to the use of fine unstructured grids and the use of small-time steps to achieve accuracy and stability.

1.1 The Eglin Test Case Model

The EGLIN test model is made up of three parts that were created using SOLIDWORKS. The first is a delta wing with a constant NACA 64A010 airfoil section and a 45°sweep, the second is a pylon

with an ogive-flat plate-ogive cross-section, and the third is a finned store body with an ogive-cylinder-ogive cross-section. The wing's trailing edge has no sweep angle and a taper ratio of 0.133. On the store are four identical fins made of a clipped delta wing of a constant NACA 0008 airfoil section with a 45° sweep. Fins have leading and trailing edge sweep angles of 60 degrees and 0 degrees, respectively. The pylon and the finned body are separated by 35.6 mm. The length and diameter of the store are 3017.5 mm and 508.1 mm, respectively. The store is ejected with enough force to begin a safe initial separation until it falls for 100 mm (the stroke of the ejector piston), after which its motion is subjected to gravity and aerodynamic forces.(E. Heim 1990) Table 1 shows the store mass, the center of mass position, inertial properties, and ejector parameters. (Sunay et al., 2013)

Mass	907.185 kg
Center of Mass	1417.3 mm (aft of STV nose)
I_{xx}	27.1163 kg-m^2
I_{yy}	488.0944 kg-m^2
I_{zz}	488.0944 kg-m^2
Forward Ejector Force	10676.01 N
Aft Ejector Force	42703.0 N
Forward Ejector Moment	-1920.0 Nm
Aft Ejector Moment	14057.0 Nm
Ejector Piston stroke length	0.10 m

Table 1. Six Degree of Freedom Parameters showing the store mass, the center of mass position, inertial properties, and ejector parameters (Riboli, n.d.)

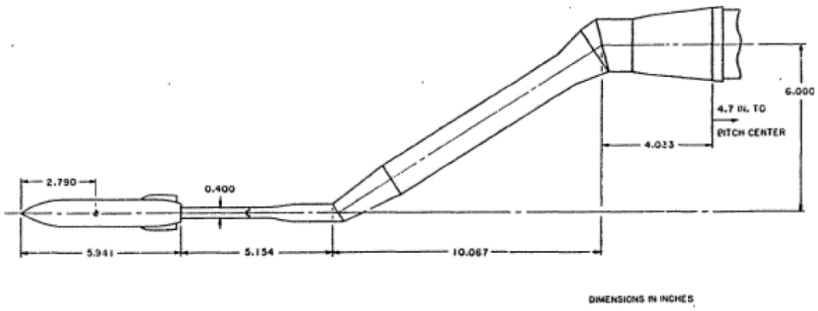

Figure 1. Sketch of the Eglin Test Case showing the dimensions in inches (E. Heim 1990)

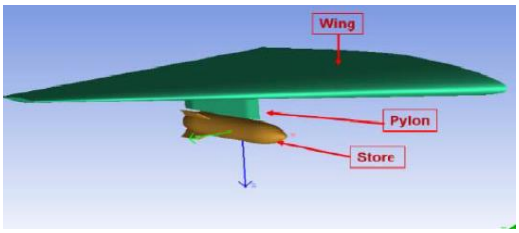

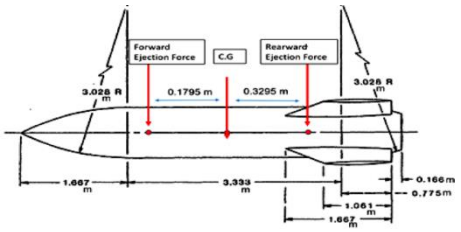

Figure 2. (left) Geometry of the wing/pylon/store(Sheharyar et al., 2018); Figure 3. (right) Dimensions of The Store(Sheharyar et al., 2018)

2. The Governing Equations

2.1 Conservation Equations

Solving potential equations, Navier-Stokes (N-S) equations could be at the heart of any CFD application. The N-S relationship describes how pressure, temperature, and density are related to a moving fluid. They consist of a set of coupled partial differential equations; one continuity equation for mass conservation, three equations for momentum conservation, and one equation for energy conservation, all of which are time dependent. Although theoretically possible, these equations are extremely difficult to solve analytically and are thus more commonly solved on computers via approximations.

Mass Conservation Equation as shown in Equation (1).

$$\frac{\partial \rho}{\partial t} + \frac{\partial}{\partial x_i} \rho u_i = 0 \tag{1}$$

Momentum Conservation Equation as shown in Equation (2).

$$\frac{\partial \rho u_i}{\partial t} + \frac{\partial u_j \rho u_i}{\partial x_j} = \frac{\partial \sigma_{ij}}{\partial x_j} + \rho g_i \tag{2}$$

Energy Conservation Equation as shown in Equation (3)

$$\frac{\partial \rho H}{\partial t} + \frac{\partial u_j \rho H}{\partial x_j} = \frac{\partial p}{\partial t} + \frac{\partial u_j p}{\partial x_j} + \sigma_{ij} \frac{\partial u_i}{\partial x_j} + \frac{\partial}{\partial x_j} K \frac{\partial T}{\partial x_j} + \dot{q} \tag{3}$$

2.2 Six Degree of Freedom Equations

To simulate flows around moving objects, scFLOW employs the ALE (Arbitrary Lagrangian-Eulerian) method,(Arbitrary Lagrangian-Eulerian Method, n.d.) which handles both the moving coordinate system and the fixed coordinate system at the same time. The effect of mesh movement is added to the equation of the fixed coordinate system in the moving region, and the fixed and moving coordinate systems are calculated simultaneously. Moving condition setting for a moving region, as well as selection and setting of the connection method for both static and moving regions, are required in the simultaneous calculation with the ALE method. By applying the moving condition to the volume region containing the object, the moving object is represented. Translation and rotation are examples of settable motions. The static and moving regions can be connected by an overset mesh.(Overset Mesh - Fluid Codes - Ansys Engineering Simulation, n.d.)

The effects of element motions are incorporated into the equations for the fixed coordinate system in ALE. The following effects are added to the fixed coordinate system's mass conservation equation and momentum equations (ScFLOW User's Guide Analysis Method, n.d.)

Mass Conservation Equation in Fixed Coordinate System as shown in Equation (4).

$$\frac{\partial \rho}{\partial t} + \frac{\partial}{\partial x_i} \rho (u_i - v_i) = 0 \tag{4}$$

Momentum Conservation Equation in Fixed Coordinate System as shown in Equation (5).

$$\frac{\partial \rho u_i}{\partial t} + \frac{\partial (u_j - v_j) \rho u_i}{\partial x_j} = \frac{\partial \sigma_{ij}}{\partial x_j} + \rho g_i \tag{5}$$

In the energy conservation (second term on the left side of the equation) must be replaced by $(u_j - v_j)$. The term v_j refers to the mesh's speed of movement.

For the combination of the moving elements, the complex movement of the object under investigation is simulated using the Six DOF Motion. The equation of motion can be used to compute the pressure and viscous stress of a fluid, as well as the motion of a rigid body to which an external force is applied. To construct the equation of motion, the mass and moment of inertia of the portion moving as the rigid body are automatically calculated from its material properties.

The Six DOF solver computes the translational and angular motion of an object's center of gravity using the object's forces and moments. In the inertial coordinate system, the governing equation for the translational motion of the center of gravity is solved.

$$\dot{\vec{v}}_G = \frac{1}{m}\sum \vec{f}_G \tag{6}$$

$\dot{\vec{v}}_G$ is the translational motion of the center of gravity, m is the mass, and $\vec{f}_G$ is the gravitational force vector. Using body coordinates, the angular motion of the object, $\dot{\vec{\omega}}_B$, is more easily computed as shown in Equation (7).

$$\dot{\vec{\omega}}_B = L^{-1}\left(\sum \vec{M}_B - \vec{\omega}_B \times L\vec{\omega}_B\right) \tag{7}$$

Here, where L is the inertia tensor, $\vec{M}_B$ is the moment vector of the body, and $\vec{\omega}_B$ is the rigid body angular velocity vector. The moments are transformed from inertial to body coordinates using Equation (8).

$$\vec{M}_B = R\vec{M}_G \tag{8}$$

As a result, the translational equation describes the aircraft in terms of its three translational degrees of freedom, whereas the rotational equation describes the aircraft in terms of its three rotational degrees of freedom. As a result, Newton's second law yields six equations for the six degrees of freedom of a rigid body. To predict the trajectory of store separation, two sets of equations, Navier-Stokes equations, and Equations of motion, must be solved concurrently.

3. CFD Modelling and Simulation

3.1 CAD Modelling

The Eglin Test Model consisting of the wing, the pylon, and the store is modeled to which an external flow domain is added which is known as the computational domain where the external flow over the model will be analyzed. The size of the computational domain must be large enough so as not to have any influence on future computations. A cylindrical domain is created on the store which is used to create overset mesh over the domain. The two meshing units of the overset mesh that are created in scFLOW are the background unit and the component unit. The background unit consists of the wing and the pylon, whereas the component unit consists of the missile body.

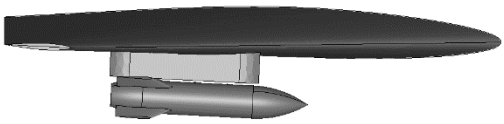

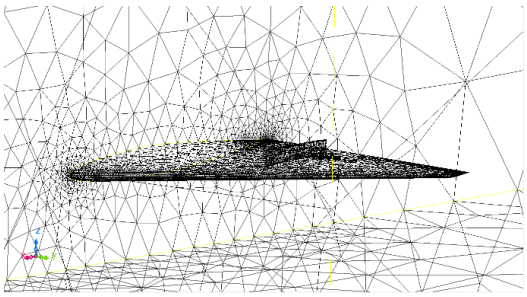

Figure 4. (left) The Eglin Model Geometry created in scFLOW; Figure 5. (right) Build Analysis Model showing tiny facet creation on the model.

scFLOW has the feature of building the analysis model out of the CAD. By doing this, several facets are created on the model which helps in removing all the unnecessary curved edges that may interfere with the solution. Since there are two components of the overset mesh that consist of the geometry, the build analysis model will be created twice, one for each unit. This group of triangle facets which are created during the build analysis model is used for subsequent mesh generation.

3.2 Material Specification and Analysis Conditions

The wing pylon body and the missile body are modeled as an obstacle. The fluid around the obstacle is modeled as the compressible air at 20 degrees Celsius

Since the flow involved in the study is compressible, the density-based solver is used. The density-

based solver solves simultaneous equations without breaking them down into conservation equations. Mass conservation solves the mass conservation problem for compressible fluids and is satisfied by rigorously tracking the density change. Because density, pressure, temperature, and velocity are all interdependent, the system of equations can be closed by adding an equation of state to each conservation equation. The turbulence model employed for this study is the standard k-EPS model. (Versteeg & Malalasekera, 1996) The k-EPS model is the 2-equation closure model which includes two additional transport equations, which are the Turbulence Kinetic Energy k and the Turbulence Dissipation Epsilon.

Parameters	Value
Mach Number	0.95
Static temperature	236.7 K
Reference Pressure	36042 Pa
Mach No.	0.95
Turbulence model	RANS, k-epsilon
Time-step	1e-04 [s]
No. of elements	2.2 million

Table 2. Flow Analysis Conditions used in the study

The steady-state calculation is performed in the initial stages of the simulation without the use of Six DOF Equations. The results of the steady-state simulations are adopted as the initialization for the transient state calculation. For this study, the steady-state simulation was run for 2000 cycles. The default temperature is set at 236.7 K. The gravity is considered in the positive Z direction as the orientation of the model and the base value of pressure is specified as equal to the absolute pressure. For the transient analysis, the time step was taken at 0.0001 and the simulation is run for a total of 0.32 seconds. (Sunay et al., 2013)

The simulation has been performed in the transonic regime. The Mach number under consideration is 0.95.(Sunay et al., 2013) At the inlet, the velocity component and the Mach number are specified. The velocity component is in the negative X direction as the inlet is registered in the same. The outlet is defined as the Static Pressure (Outflow) where the pressure value is specified as 36042 Pa. The top, bottom, and ymax are defined as the ‘free slip’ wall boundary condition.

3.3 Coupling using Six Degree of Freedom

The computations begin at t = 0s to obtain the aerodynamic forces and moments, and then the solver is coupled with a 6-DOF code to predict the entire store trajectory using the quasi-steady approach. The store is subjected to both forward and aft ejector forces, which are turned off once the ejector stroke lengths are exceeded. The expectation for the results by applying these ejector forces is that for a real-time of t = 0.06 seconds, the store pitches up due to ejector forces acting on it. After the effect of the ejector forces fades, aerodynamic forces acting on the store take control, resulting in a pitch-down moment.(Osman et al., n.d.) The Six DOF Parameters are shown in Table 1. The forward and the rearward ejector force is applied in the tabular format according to their working since the ejector forces act for 0.06 s and then stop.

3.4 Analysis Control Methods

To set the under-relaxation coefficient, for the system of equations of the density-based solver, a 0.2 value has been specified. The under-relaxation coefficient for the equations of density-based solver and turbulence and diffusion is set as 0.2,0.7 and 0.99 respectively. Second-order accuracy with limiter is used for the Accuracy of the convective terms for the mass, momentum, energy, turbulence, and the diffusion equation. First Order Accuracy of Time Derivative is used. The Least

Square Method is used for Gradient Calculation.

3.5 Mesh

Elements are placed in a region to analyse physical phenomena and calculate changes in physical quantity. scFLOW includes a polyhedral mesher (arbitrary polyhedrons) to improve the cell-centered Solver's stability and calculation accuracy. This is an automatic mesher that will generate mesh based on the number of elements specified, making mesh fine near the wall surface where a rapid flow change is anticipated. The mesh generation involves the creation of octree and the generation of the polyhedral mesh along with the prism layers which are inserted along the wall.

Due to the use of the overset mesh, the octree creation also takes place separately for each of these units. For the first meshing unit, the minimum octant size for all the surfaces is given as 12.8 and the maximum octant size is also of the same value. Since there is space in the far-field, octants are coarsened up to this size, which is the maximum octant size. The octant refinement level is specified from the near-wall up to the far-field. For the second meshing unit, the minimum and the maximum octant size are specified as 0.1, for the same reasons stated above. The number of elements generated for meshing units 1 and 2, while creating the octree is 2,254,965 and 280,709 respectively.

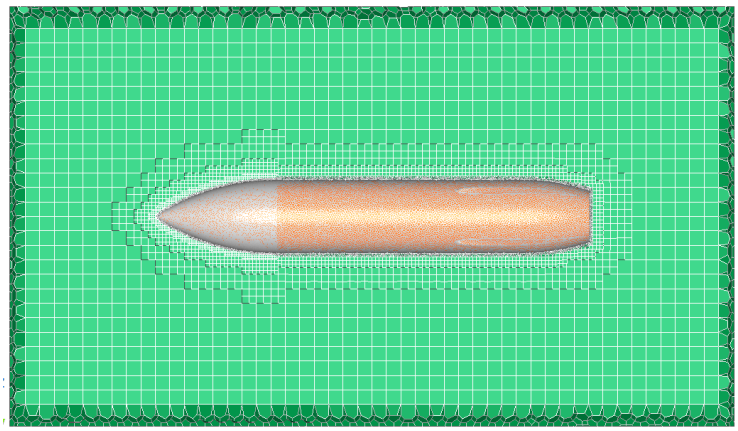

Figure **Error! No text of specified style in document.**. Meshed missile body showing prism layer along the walls and polyhedral (unstructured) mesh generation

scFLOW automatically provides the creation of the prism layer along the walls. Since The distance from the wall is not uniform without the prism elements, sufficient accuracy cannot be obtained for velocity and temperature gradient. However, with the prism elements, the distance from the wall becomes uniform. Sufficient accuracy can be obtained for velocity and temperature gradient as well as the prism layer has the advantage for both calculation accuracy and stability. Here the prism layer is generated along the walls of the wing, the pylon, and the store. The number of prism layers specified here is 2 and the thickness of the prism layer is 0.2. As the polyhedral which is an unstructured mesh is generated, the final count of the number of elements is 2,201,265.

4. Analysis Results

4.1 Linear Displacement versus Time Graph

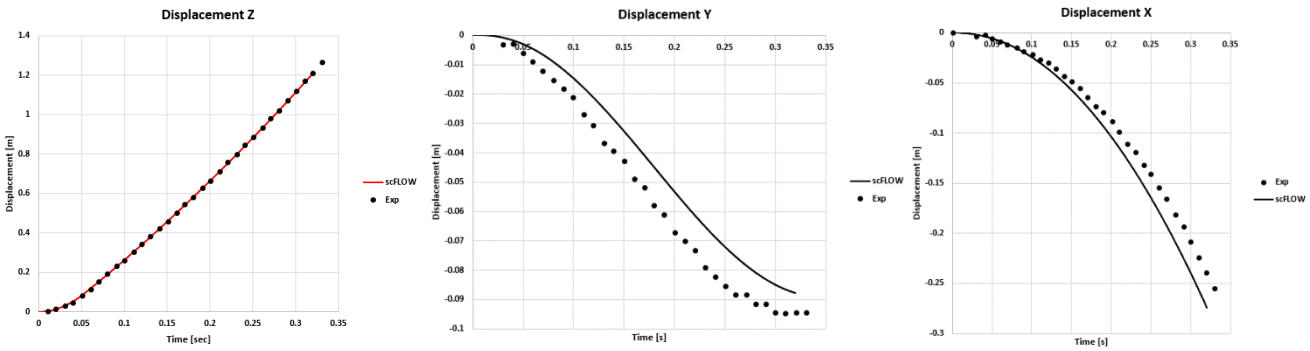

Figure 7(a) Figure 7(b) Figure 7(c)

Figure 7(a-c). Linear Displacement versus Time graph in X, Y and Z direction comparing the numerical and the experimental data

When the ejector forces act, the store separation initiates. At ejection initiation, the ejector forces are applied to the store. When the store separates from the aircraft due to gravity and ejector forces, it begins to move backward, downward, and inward. After about t=0.2 seconds, the inward and backward movements begin as shown in Figure 9.

X, Y, and Z translations of the store are shown in Figure 7(a-c). The Z translation appears to closely match the experimental data for the rigid wing. A small difference in X trajectory and Y trajectory was observed. This is because the ejector and gravity forces outweigh the aerodynamic forces in the Z direction. The small difference in horizontal displacement is to be expected because drag is understated due to viscous effects.

4.2 Angular Displacement versus Time Graph

Figure 8(a-c) compares the store trajectory for the center of gravity angular orientations with respect to time for the experimental and numerical case. Since the aerodynamic forces prevail, the store moves in a pitch-up, negative yaw, and positive roll direction.

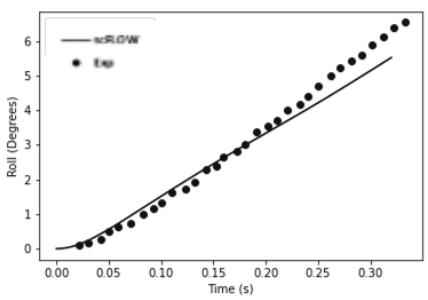

Figure 8(a)

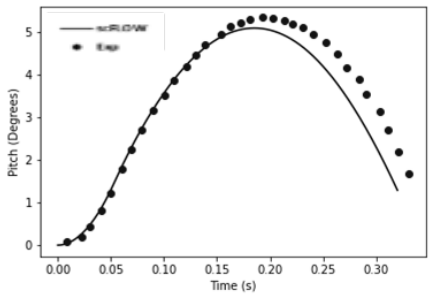

Figure 8(b)

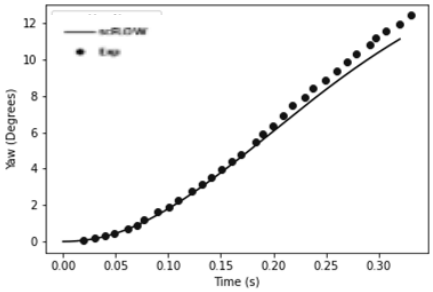

Figure 8(c)

Figure 8(a-c). Roll, Pitch, and Yaw versus time graph comparing the numerical and the experimental data

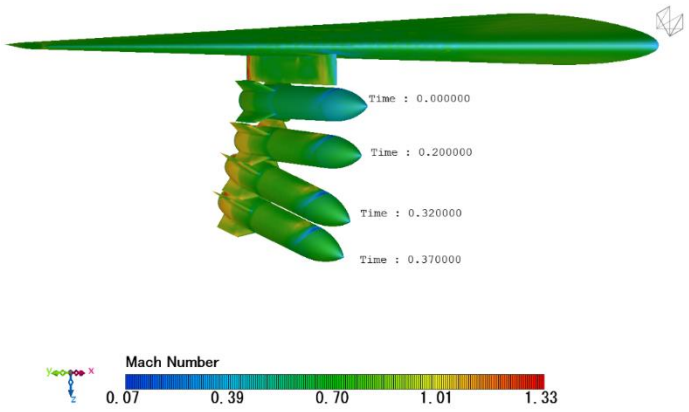

Figure 9. The Store Separation with Event Ejectors at Mach 0.95

In Figure 8(a), the numerical roll trend shows a similar trend to the experimental data. Although the trend is very similar, the results show a minor deviation from the experimental data. This deviation is seen after 0.05 second which is when the ejector forces also disappear.

In Figure 8(b), the pitching trend is very close to the experimental data. Since the aerodynamic forces and the ejection forces exist, the store first moves in a pitch up direction. When the ejector forces disappear, the motion of the store results in a pitch down movement.

In Figure 8(c), the yaw orientation shows similarity in trend when compared to the experimental data. Minor deviations occur near time 0.30 seconds.

5. Conclusion

The study performed using the Eglin Test Model at Transonic Mach Number using scFLOW

successfully predicts the influence of ejector and gravity forces on the store trajectory which overcomes the aerodynamic force. The linear displacement in the z direction matches very well with the experimental data. Also, the pitch orientation shows a good agreement. The ease of use of Overset Mesh in scFLOW enables the ease of application of Six DOF feature for coupling with the Navier – Stokes Equation. Software Cradle provides a very comprehensive way of post processing that enables easy analysis of results.

Acknowledgment

A token of gratitude to Dr. Rajesh Yadav, Assistant Professor, University of Petroleum and Energy Studies for his support. Also, would like to thank Hexagon Manufacturing Intelligence, India for providing this opportunity to conduct the study.

References

Arbitrary Lagrangian-Eulerian Method. (n.d.). Retrieved May 9, 2022, from http://www.me.sc.edu/research/jzuo/Contents/ALE/ALE_1.htm

Demir, H. Ö., Selimhocaoğlu, B. T., & Alemdaroğlu, N. (n.d.). CFD Applications in Store Separation Görkem DEMİR.

E. HEIM, "CFD Wing/Pylon/Finned Store Mutual Interference Wind Tunnel Experiment", Arnold Engineering Development Center, AD-B152 669, September 10-17, 1990

Madasamy S, Thilagapathy G, & Arulalagan R. (2016). Investigation of Store Separation and Trajectory of Weapons in Military Aircraft. International Journal of Scientific & Engineering Research, 7(2). http://www.ijser.org

Osman, A. A., Bayoumy Aly, A. M., El, I., Abdellatif, O. E., & Khallil, E. E. (n.d.). Investigation of the Effect of Grid Size on External Store Separation Trajectory using CFD.

Overset Mesh - Fluid Codes - Ansys Engineering Simulation. (n.d.). Retrieved May 9, 2022, from https://fluidcodes.com/software/overset-mesh/

Panagiotopoulos, E. E., & Kyparissis, S. D. (n.d.). CFD Transonic Store Separation Trajectory Predictions with Comparison to Wind Tunnel Investigations.

Riboli, F. M. (n.d.). Store Separation Predictions for Weapon Integration on a Fighter-Type Aircraft Safe Separation Simulation View project. https://www.researchgate.net/publication/346714232

scFLOW User's Guide Analysis Method - 04/Nov/2021. (n.d.).

Sheharyar, M., Uddin, E., Ali, Z., Zaheer, Q., & Mubashar, A. (2018). Simulation of a standard store separated from generic wing. Journal of Applied Fluid Mechanics, 11(6), 1579–1589. https://doi.org/10.29252/jafm.11.06.28865

Sunay, Y. E., Gülay, E., & Akgül, A. (2013). Numerical Simulations of Store SeparationTrajectories Using the EGLIN Test. In Scientific Technical Review (Vol. 63, Issue 1).

Versteeg, H. K., & Malalasekera, W. (1996). An introduction to computational fluid dynamics: the finite volume method, 1995. Harlow-Longman Scientific & Technical, London, M, 503.